0026-895X/09/7505-1062–1073$20.00
MOLECULAR PHARMACOLOGY
Vol. 75, No. 5
52829/3460539
Mol Pharmacol 75:1062–1073, 2009
Printed in U.S.A.

The Four Major N- and C-Terminal Splice Variants of the Excitatory Amino Acid Transporter GLT-1 Form Cell Surface Homomeric and Heteromeric Assemblies[S]

Eleanor Peacey, Christopher C. J. Miller, John Dunlop, and Marcus Rattray

Wolfson Centre for Age-Related Diseases (E.P., M.R.) and MRC Centre for Neurodegeneration Research, Institute of Psychiatry (C.C.J.M.), King's College London, London, United Kingdom; Discovery Neuroscience, Wyeth Research, Princeton, New Jersey (J.D.); and Reading School of Pharmacy, University of Reading, Reading, United Kingdom (M.R.)

Received October 15, 2008; accepted February 6, 2009

ABSTRACT

The L-glutamate transporter GLT-1 is an abundant central nervous system (CNS) membrane protein of the excitatory amino acid transporter (EAAT) family that controls extracellular L-glutamate levels and is important in limiting excitotoxic neuronal death. Using reverse transcription-polymerase chain reaction, we have determined that four mRNAs encoding GLT-1 exist in mouse brain, with the potential to encode four GLT-1 isoforms that differ in their N and C termini. We expressed all four isoforms (termed MAST-KREK, MPK-KREK, MAST-DIETCI, and MPK-DIETCI according to amino acid sequence) in a range of cell lines and primary astrocytes and show that each isoform can reach the cell surface. In transfected human embryonic kidney (HEK) 293 or COS-7 cells, all four isoforms support high-affinity sodium-dependent L-glutamate uptake with identical pharmacological and kinetic properties. Inserting a viral epitope (tagged with V5, hemagglutinin, or FLAG) into the second extracellular domain of each isoform allowed coimmunoprecipitation and time-resolved Förster resonance energy transfer (tr-FRET) studies using transfected HEK-293 cells. Here we show for the first time that each of the four isoforms is able to combine to form homomeric and heteromeric assemblies, each of which is expressed at the cell surface of primary astrocytes. After activation of protein kinase C by phorbol ester, V5-tagged GLT-1 is rapidly removed from the cell surface of HEK-293 cells and degraded. This study provides direct biochemical evidence for oligomeric assembly of GLT-1 and reports the development of novel tools to provide insight into the trafficking of GLT-1.

GLT-1 (the human homolog of which is EAAT2) is the predominant excitatory amino acid transporter in the CNS, mediating up to 95% of the total sodium-dependent glutamate uptake (Danbolt et al., 1992; Haugeto et al., 1996; Tanaka et al., 1997). GLT-1 is predominantly expressed on astrocytes, and its main functions are to regulate synaptic glutamate levels and to prevent excitotoxic neuronal death as a result of prolonged excitation of glutamate receptors (Danbolt, 2001; Rattray and Bendotti, 2006). GLT-1 is a multi membrane-spanning protein that, on the basis of biochemical analyses, has been suggested to exist as a multimer (Haugeto et al., 1996; Gendreau et al., 2004). This concept has been strengthened after the resolution of the crystal structure of a bacterial homolog of GLT-1 that reveals a trimeric structure (Yernool et al., 2004).

In recent years, a number of splice variants of GLT-1 have been described (Table 1) that, where tested, have human homologs in the EAAT2 gene. At the 3′ end of the *GLT-1* gene, alternative exon use can result in the generation of at least three distinct C-termini. Immunoreactivity against each of the three different C termini has been demonstrated to be present in the CNS (Rothstein et al., 1994; Schmitt et al., 2002; Rauen et al., 2004). In addition, at the 5′ end of the

This work was supported by the Medical Research Council [Doctoral Training Grant and Grant G0501573]; the Motor Neuron Disease Association [UK: USA collaborative award]; and the Wellcome Trust [Grant 078662].
Article, publication date, and citation information can be found at http://molpharm.aspetjournals.org.
doi:10.1124/mol.108.052829.
[S] The online version of this article (available at http://molpharm.aspetjournals.org) contains supplemental material.

ABBREVIATIONS: GLT-1, glutamate transporter-1; CNS, central nervous system; ALS, amyotrophic lateral sclerosis; HA, hemagglutinin; PCR, polymerase chain reaction; FBS, fetal bovine serum; PMSF, phenylmethylsulfonyl fluoride; TBS, Tris-buffered saline; TTBS, Tris-buffered saline/Tween 20; HBS, HEPES-buffered saline solution; WAY-213394, N^4-(2′-methyl-1,1′-biphenyl-4-yl)-L-asparagine; WAY-213613, N^4-[4-(2-bromo-4,5-difluorophenoxy) phenyl]-L-asparagine; WAY-212922, N^4-[7-(trifluoromethyl)-9*H*-fluoren-2-yl]-L-asparagine; WAY-144855, 3-amino-tricyclo[2.2.1.$0^{2.6}$]heptane-1,3-dicarboxylic acid; NGS, normal goat serum; HEK, human embryonic kidney; PBS, phosphate-buffered saline; PMA, phorbol 12-myristate 13-acetate; IC, intracellular; M, membrane; ANOVA, analysis of variance; tr-FRET, time-resolved Förster resonance energy transfer; PKC, protein kinase C; SOD1, superoxide dismutase-1; GFP, green fluorescent protein; EAAT, excitatory amino acid transporter.

gene, there is extensive differential exon use predicted to result in at least four distinct N termini (Utsunomiya-Tate et al., 1997; Münch et al., 2002; Rozyczka and Engele, 2005), although which N termini are expressed in the CNS in vivo has not yet been established. Thus, at least 12 isoforms of GLT-1 potentially exist, depending on the exact splicing around the 5′ and 3′ ends of the coding sequence.

Because GLT-1 can exist as an oligomeric assembly, then isoforms may combine to form homomers or heteromers, raising the possibility that there are a large number of different GLT-1 multimers, with distinct functional properties. Not only is it not yet known whether or not heteromers can exist, but there is little direct evidence to address whether there are functional differences between GLT-1 isoforms. GLT-1 isoforms that differ in their C termini (KREK or 1a and DIETCI or 1b/v) have been compared and show no functional differences in transport activity (Utsunomiya-Tate et al., 1997; Chen et al., 2002; Sullivan et al., 2004). However, a detailed comparison of all important mammalian isoforms that differ in their N and C termini has not been made.

In some neurodegenerative diseases or CNS injury states, there is an alteration of relative expression of GLT-1 isoforms. For example, Münch et al. (2002) showed increased expression of a transcript containing the "5UT4" exon, predicting that alternatively spliced GLT-1 isoforms bearing an N terminus with the initial amino acid residues MPK may be relatively up-regulated in a mouse model of amyotrophic lateral sclerosis (ALS). Furthermore, they proposed that the MPK isoform(s) may contribute to down-regulation of functional GLT-1. Yi et al. (2005) showed a decrease of GLT-1 containing the DIETCI C terminus in a model of traumatic brain injury, and in a piglet model of hypoxia, there is a relative loss of isoforms containing the KREK C terminus without loss of DIETCI immunoreactivity (Pow et al., 2004). Given the importance of GLT-1 in neuroprotection, these findings suggest that the relative changes in levels of different GLT-1 isoforms may have functional implications. Some isoforms or multimeric combinations of isoforms may be more effective in limiting neuronal injury resulting from increased glutamate levels, for example by having a higher rate of glutamate uptake or possessing increased stability in the plasma membrane.

We set out to determine the function and multimerization of mouse GLT-1 isoforms. We first identified which GLT-1 isoforms are the most abundantly expressed at the mRNA level and then produced epitope-tagged GLT-1 isoform cDNA constructs to enable the cell surface expression, multimerization, and pharmacological properties of GLT-1 to be determined. Furthermore, we report the use of these constructs in in vitro assay systems to assess the regulation of cell-surface expression of GLT-1 by the protein kinase C activator, phorbol ester.

Materials and Methods

RT-PCR, cDNA Constructs, and Epitope Tagging. Total RNA was extracted from mouse frontal cortex using RNABee reagent, and reversed transcribed into cDNA. Mouse GLT-1 splice variant cDNAs were obtained by PCR using oligonucleotide primers (Sigma Aldrich, Poole, UK) against regions common to all splice variants or specific to the N- or C-terminal sequences (primer sequences in Supplemental Table 1). Twenty-five-microliter reactions contained 0.2 μM forward primer, 0.2 μM reverse primer, 2.5 μl of cDNA, 0.2 units/μl Platinum *Taq* high fidelity (Invitrogen, Paisley, UK), 0.2 mM dNTPs, and 2 mM $MgSO_4$ in 1× buffer (60 mM Tris-SO_4, pH 8.9, 18 mM ammonium sulfate; Invitrogen). Amplification was performed for 35 cycles (94°C for 30 s, 55°C for 30 s, then 68°C for 110 s) followed by a final extension period at 68°C for 7 min. Full-length cDNA PCR products for each splice variant of GLT-1 were ligated into the plasmid pCR2.1 then subcloned into pcDNA3.1- (Invitrogen) and sequenced (Molecular Biology Unit, King's College, London, UK). Sequences coding for the V5 (GKPIPNPLLGLDST), hemagglutinin (HA; YPYDVPDYA), or FLAG (DYKDDDDK) epitope tags were inserted into the region of cDNA encoding the large extracellular loop of the transporter (between Pro^{199} and Pro^{200}) using a two-step PCR method with overhanging primers (adapted from Zeng et al., 2004). The resulting PCR products were re-introduced into the GLT-1 sequences between the BbvCI and BsrGI restriction sites.

Cell Culture and Transient Transfections. All cells were maintained in 95% O_2/5% CO_2 at 37°C. COS-7 and HEK-293 cells were grown in Dulbecco's modified Eagle's medium containing 2 mM L-glutamine, 4500 mg/liter D-glucose, and 110 mg/liter sodium pyruvate, supplemented with 10% heat-inactivated fetal bovine serum (FBS), 100 units/ml penicillin, and 100 μg/ml streptomycin. Primary cortical astrocytes were prepared from 15- to 16-day-old NIH Swiss mouse embryos (Harlan, Bicester, Oxon, UK) as previously described (Tortarolo et al., 2004) and plated at 10^6 cells/ml into 24-well plates containing 13-mm round glass coverslips coated with 1.5 μg/ml poly-L-ornithine and 2 μg/ml laminin. Cells for transient expression studies at 90 to 100% confluence were transfected with cDNAs using Lipofectamine 2000 reagent (Invitrogen) for 6 h. cDNAs used encoded the GLT-1 splice variants, or histamine H_4 receptors (kind gifts of Dr. Paul Chazot, University of Durham, UK). COS-7 and HEK-293 cells were used 24 h after transfection.

Western Blotting. Total cell proteins were extracted at 4°C using lysis buffer (50 mM Tris, pH 7.5, 150 mM NaCl, 1% Triton X-100, 2 mM EDTA, 2 mM EGTA, 0.5 mM PMSF, 10 μg/ml leupeptin, 2 μg/ml pepstatin A, 50 mM NaF, 1 μg/ml chymostatin, 5 mM $Na_4P_2O_7$, and

TABLE 1
Mammalian GLT-1 splice variants differ in N- and C-terminal sequences.

Predicted N-Terminal Amino Acid Sequence	Predicted C-Terminal Amino Acid Sequence	Species Characterized
MASTEGANNMPK	DECKVTLAANGKSADCSVEEEPW**KREK**	Mouse (Utsunomiya-Tate et al., 1997); rat (Pines et al., 1992); human (Arriza et al., 1994)
MASTEGANNMPK	DECKVPFPFL**DIETCI**	Mouse (Utsunomiya-Tate et al., 1997); rat, termed GLT1b (Chen et al., 2002) or GLT1v (Schmitt et al., 2002)
MVSANNMPK	DECKVTLAANGKSADCSVEEEPW**KREK**	Mouse (Utsunomiya-Tate et al., 1997), termed mGLT-1A
MVSANNMPK	DECKVPFPFL**DIETCI**	Mouse (Utsunomiya-Tate et al., 1997), termed mGLT-1B; rat (Pollard and McGivan, 2000)
Undetermined	DECKSLHYVEYQ**SWV**	Rat (Rauen et al., 2004), termed GLT1c
MPK	Undetermined	Mouse (Münch et al., 2002); rat (Rozyczka and Engele, 2005)
MKRPKEHSIQRSANNMPK	Undetermined	Rat (Rozyczka and Engele, 2005)

1 mM Na_3VO_4). Samples were centrifuged at 578*g* for 5 min, and protein concentration of the supernatant was determined using the protein assay dye reagent concentrate (Bio-Rad Laboratories, Hercules, CA). Protein (30 μg) was diluted with Laemmli buffer (final concentration, 62.5 mM Tris, pH 6.8, 2% SDS, 10% glycerol, 5% mercaptoethanol, and 0.0025% bromphenol blue), and separated by SDS-polyacrylamide gel electrophoresis on 9% polyacrylamide gels without boiling. Proteins were transferred onto nitrocellulose membrane (GE Healthcare, Chalfont St. Giles, Buckinghamshire, UK). Membranes were blocked in Tris-buffered saline (TBS) containing 4% skimmed milk powder for 40 min, washed twice in TTBS [TBS supplemented with 0.05% (v/v) Tween 20] and incubated overnight at 4°C with primary antibody diluted in TTBS containing 1% nonfat dry milk. The anti-GLT-1 antibody, B12, was a kind gift of Prof. N. Danbolt (University of Oslo, Oslo, Norway) and was used at 1:5000, the anti-V5 antibody (Invitrogen) was used at 1:5000, anti-HA (Roche, Burgess Hill, UK) was used at 1:1000, the anti-FLAG antibody (Sigma) was used at 1:5000, and the anti-actin antibody (Abcam plc, Cambridge, UK) was used at 1:500,000. Membranes were then washed twice in TTBS and incubated for 45 min at room temperature with HRP-conjugated secondary antibody diluted in TTBS containing 1% skimmed milk powder [anti-rabbit (Sigma) used at 1:1000; anti-mouse (Vector Laboratories, Peterborough, UK) used at 1:1000; anti-rat (Sigma) used at 1:7000]. Membranes were then washed twice in TTBS and once in TBS. Protein bands were detected using the ECL detection system with Hyperfilm ECL (GE Healthcare).

[^{3}H]L-Glutamate Uptake. COS-7 cells were seeded 48 h before the assay at a density of 2×10^5 cells/well, and transfected with GLT-1 splice variant cDNA 24 h before the assay. Stably transfected HEK-293 cells, which were selected for stable expression of GLT-1 isoforms and maintained in Dulbecco's modified Eagle's medium supplemented with 10% FBS, 10 units/ml penicillin, 10 μg/ml streptomycin, and 400 μg/ml G-418 (Geneticin), were seeded 24 h before the assay at a density of 2×10^5 cells/well. Twenty-four-well culture plates used for uptake assays were precoated in 10 μg/ml poly-D-lysine. All incubations were done in HEPES-buffered saline solution (HBS; 5 mM Tris base, pH 7.4, 10 mM HEPES, 140 mM NaCl, 2.5 mM KCl, 1.2 mM $CaCl_2$, 1.2 mM $MgCl_2$, 1.2 mM K_2HPO_4, and 10 mM glucose). Cells were washed twice with Na^+-free HBS (prepared by equimolar replacement of Na^+ with choline) at room temperature, then incubated with 3 to 115 μM L-glutamate (containing 1 μCi/ml [^{3}H]L-glutamate) in HBS at room temperature for 8 min. Under these conditions, [^{3}H]L-glutamate uptake was shown to be linear up to 20 min (results not shown). In transfected COS-7 cells, data with [^{3}H]L-glutamate uptake was essentially identical to data obtained using [^{3}H]D-aspartate uptake, suggesting that metabolism of L-glutamate or tritium exchange was negligible under these conditions. For each assay, parallel determinations were performed using Na^+-free HBS. Assays were stopped by aspiration followed by two washes with ice-cold Na^+-free HBS. Cells were lysed in 0.1 M NaOH and accumulated radioactivity measured (Winspectral 1414 liquid scintillation counter; PerkinElmer Life and Analytical Sciences). For pharmacological characterization, HEK-293 cells stably expressing various constructs were incubated in HBS containing Na^+ and 50 nM [^{3}H]L-glutamate ± inhibitor compounds (1 nM–10 mM) at room temperature for 8 min. Inhibitor compounds used were WAY-213394, WAY-213613, WAY-212922, and WAY-144855, all kind gifts of Dr. John Dunlop (Wyeth Research, NJ) (Dunlop et al., 2005), DL-*threo*-β-benzyloxyaspartate, dihydrokainate, kainate, (±)-*threo*-3-methylglutamate, *threo*-β-hydroxyaspartate; L-transpyrrolidine-2,4-dicarboxylic acid, 2*S*,1′*S*,2′*R*-2-(carboxycyclopropyl)glycine, all from Tocris (Bristol, UK), and L-serine-*O*-sulfate (Sigma Aldrich), all reviewed by Bridges and Esslinger (2005). For each assay, parallel determinations were performed using Na^+-free HBS containing 50 nM [^{3}H]L-glutamate but no inhibitors.

Immunofluorescence. Cells on glass coverslips were washed twice with PBS and fixed in 4% paraformaldehyde for 30 min. Cells were washed three times with PBS before blocking for 30 min with 1% (v/v) normal goat serum (NGS) in PBS. Cells were incubated with anti-V5 antibody (1:500) and/or anti-HA antibody (1:100) for 1 h in PBS containing 1% NGS. Cells were washed three times in PBS, followed by 90-min incubation with anti-rabbit Alexa Fluor 568, anti-mouse Alexa Fluor 568, or anti-mouse Alexa Fluor 488 (1:500; Invitrogen). Cells were washed three times in PBS before mounting using Mowiol antifade mountant containing the nuclear stain Hoechst 33342 (0.5 μM). Cells were visualized and images captured simultaneously in the red, green, and blue channels using a Carl Zeiss Axioplan 2 microscope rig with Axiovision Imaging software (Carl Zeiss GmbH, Jena, Germany).

A two-step immunofluorescence protocol was employed to differentiate between cell surface and intracellular populations of V5-tagged GLT-1. The V5 epitope expressed at the cell surface of fixed, unpermeabilized cells was detected as described above using the anti-V5 primary antibody and a secondary antibody conjugated to Alexa Fluor 488 (green). Cells were washed three times in PBS and then incubated with an unconjugated anti-mouse secondary antibody (Zymed Laboratories, South San Francisco, CA) to block any remaining primary antibody binding sites at the cell surface. The cells were then washed again and post-fixed in 4% paraformaldehyde. After washing, the cells were blocked and permeabilized in PBS containing 1% NGS and 0.2% Triton X-100. Another round of primary (anti-V5) and secondary (Alexa Fluor 568, red) antibodies was used to detect intracellular V5. The cells were then washed and mounted as described above.

Coimmunoprecipitation. HEK-293 cells were transfected 24 h before the coimmunoprecipitation assay with pairs of epitope-tagged GLT-1 splice variants. Immediately before the assay, cells were rinsed twice with PBS and lysed in solubilization buffer (10 mM HEPES pH 7.5, 145 mM NaCl, 0.1 mM $MgCl_2$, 1% Triton X-100, 1 mM EGTA, 1 mM PMSF, 1 mM Na_3VO_4, 1 mM NaF, 1 μg/ml aprotinin, 1 μg/ml leupeptin, and 1 μg/ml pepstatin A). These detergent-solubilized extracts were centrifuged at 100,000*g* at 4°C and supernatants diluted in solubilization buffer to achieve a final concentration of 1 mg/ml protein and 0.5% Triton X-100. Samples were precleared by incubation with 20 μl of protein A/G agarose (Calbiochem, La Jolla, CA) on a rotating mixer for 30 min at 4°C, then centrifuged at 317 *g* for 2 min. Supernatants were incubated with 2.5 μg of anti-V5 antibody (Invitrogen) or mouse myeloma IgG_{2A} (Invitrogen) overnight on a rotor at 4°C. Protein A/G agarose (37.5 μl) was added, and samples were incubated on a rotor for 1 h at 37°C. Pellets were collected by centrifugation at 317*g* for 1 min and washed three times with 1 ml of solubilization buffer containing 0.5% Triton X-100. Precipitated proteins were eluted by incubation with 100 μl of 1× Laemmli buffer on a rotor at room temperature for 30 min, then heated to 95°C for 4 min. Lysates (30 μl) and immunoprecipitates (15 μl for V5 probe or 60 μl for HA probe) were analyzed by Western blot.

Time-Resolved Förster Resonance Energy Transfer. HEK-293 cells were transfected with cDNA encoding the FLAG- or HA-tagged GLT-1 splice variants or histamine H_4 receptors, or cotransfected with two constructs. Twenty-four hours after transfection, intact cells were harvested in ice-cold PBS then pelleted by centrifugation at 162*g* for 5 min and resuspended at a concentration of 20×10^6 cells/ml in PBS containing FBS [50% (v/v)]. Aliquots of 4×10^6 cells were incubated for 4 h at room temperature with 5 nM Eu^{3+}-labeled anti-FLAG and 15 nM XL-665-labeled anti-HA (Cisbio International, Bagnols, France). Samples consisting of cells pooled from separate transfections were processed in parallel to cotransfected cells. Negative controls, which were incubated with the donor fluorophore only, were included for every sample. Cells were then pelleted by centrifugation at 714*g* for 2 min, and washed twice with 200 μl of PBS. Cells were resuspended in 200 μl of PBS and transferred to a white opaque 96-well plate. Energy transfer between the donor and acceptor fluorophores was measured by excitation at 313 nm and detection of emission at 665 and 320 nm for 450 μs after a 50-μs

delay, using a FlexStation3 plate reader (Molecular Devices, Sunnyvale, CA).

Surface Biotinylation. V5-MPK-DIETCI (GLT-1)/HEK-293 cells were treated with 100 nM phorbol 12-myristate 13-acetate (PMA) in normal growth media for 10, 30, or 60 min at 37°C, or subjected to a DMSO control. Cells were rinsed twice at 37°C in PBS/Ca^{2+}/Mg^{2+} (138 mM NaCl, 2.7 mM KCl, 1.5 mM KH_2PO_4, 9.6 mM Na_2HPO_4, 1 mM $MgCl_2$, and 0.1 mM $CaCl_2$), then incubated with freshly prepared 1 mg/ml sulfo-NHS biotin (Pierce, Rockford, IL) at 4°C for 20 min. The biotinylation solution was removed, and cells were rinsed twice with PBS/Ca^{2+}/Mg^{2+} (as above) containing 100 mM glycine and followed by a 45-min incubation in this solution at 4°C. Cells were lysed in radioimmunoprecipitation assay buffer (100 mM Tris-HCl, pH 7.4, 150 mM NaCl, 1 mM EDTA, 1% Triton X-100, 1% sodium deoxycholate, 0.1% SDS, 1 μg/ml leupeptin, 1 μg/ml aprotinin, and 250 μM PMSF). Lysates were incubated at 4°C for 60 min on a plate shaker, and then centrifuged at 17,860 g for 20 min at 4°C. Of the supernatant fraction, 40% of the volume was retained and frozen (total fraction), and 60% of the volume was incubated with an equal volume of immunopure immobilized monomeric avidin beads (Pierce) on a rotating mixer at room temperature for 60 min. The samples were then centrifuged at 17,860*g* for 5 min at 4°C. The supernatant was retained and frozen (intracellular fraction). The beads were then washed three times with 80 μl of RIPA buffer. Cell surface proteins were eluted from the avidin-biotin complex by incubation with Laemmli buffer on a rotating mixer for 30 min at room temperature, then heating to 95°C for 5 min. The total and intracellular fractions were also diluted with Laemmli buffer. Samples (12.5 μl of total lysate, 10 μl of the cell surface membrane fraction, and 25 μl of the intracellular fraction) were analyzed by Western blot.

Data Analysis. Throughout the article, numerical values, where shown, are the mean of the number of independent experiments with S.E.M. Quantification of band intensities from Western blots for cell surface biotinylation studies was performed using ImageJ (http://rsbweb.nih.gov/ij/) and data analyzed using Prism (GraphPad Software, San Diego, CA). Band intensities were normalized to compare data from three independent experiments. For each of the total lysate samples, the band intensities for the glycosylated monomeric and multimeric bands were added, and this value was expressed as a percentage of the summed band intensities for all total lysate samples from that film. To determine the relative intracellular distribution of GLT-1, the cell surface membrane (M) fraction and intracellular (IC) fractions were calculated as M/(M + IC) and IC/(M + IC) respectively. Significant differences in total expression were determined using one-way ANOVA with the Bonferroni post hoc test. P values <0.05 were considered statistically significant.

For [^{3}H]L-glutamate uptake studies, the rate of Na^+-dependent uptake was calculated in pmol · mg^{-1} · min^{-1}, and regression lines were fitted to one-site saturation curves. K_m and V_{max} were determined from Eadie-Hofstee transformation of the saturation data. At least three independent experiments were performed and data analyzed using GraphPad Prism. Differences in K_m or V_{max} were tested for significance using one-way ANOVA with the Bonferroni post hoc test. Uptake in the presence of transport inhibitors was calculated as percentage of maximum Na^+-dependent uptake in the absence of inhibitor. Sigmoidal dose-response curves were fitted to the log concentration-response graphs and IC_{50} values were calculated. Statistical significance was determined using one-way ANOVA with the Bonferroni post hoc test (Prism).

For tr-FRET studies, fluorescence detected at 620 nm was defined as the total Eu^{3+} (donor) signal. The fluorescent signal from PBS at 620 and 665 nm was subtracted from the values and the ratio R = [(fluorescence at 665/fluorescence at 620) × 10^4] was calculated. The specific signal over background was then determined using the formula: $\Delta F = (R_{pos} - R_{neg})/(R_{neg})$, where R_{pos} corresponds to the ratio of fluorescence for the samples, and R_{neg} corresponds to the ratio of energy transfer for the negative control (incubated with the donor fluorophore only). Data were analyzed using GraphPad Prism. Significant differences in total expression were determined using one-way ANOVA with the Bonferroni post hoc test. P values <0.05 were considered statistically significant.

Results

Expression of mRNAs Encoding GLT-1 Isoforms in Mouse CNS. The different predicted N- and C-terminal splice variants for mouse GLT-1 are shown in Table 1. To determine whether each of the 12 possible isoforms is expressed, RT-PCR was used to determine the presence of mRNAs encoding each of these putative GLT-1 variants using specific primers (primers are listed in Supplemental Table 1). RT-PCR was performed on cDNA prepared from adult mouse cerebral cortex, using primers against a region common to all splice variants, or primers specific for each N- or C-terminal splice variant (Fig. 1). Of the N-terminal variants, transcripts containing exons encoding MAST and MPK N termini are abundant, but transcripts containing sequences leading to MVS and MKRP N termini are not found. The MVS N-terminal splice variant was successfully amplified from mouse liver cDNA (result not shown). Of the C termini, variants encoding the DIETCI and KREK C termini are abundant, and transcripts encoding variants with the SWV C terminus are found only at low levels. Using RT-PCR, full-length mRNAs encoding four of the twelve possible isoforms are found to be expressed at detectable levels (Fig. 1). We henceforth refer to these four most abundant GLT-1 isoforms as MAST-DIETCI, MAST-KREK, MPK-DIETCI, and MPK-KREK according to the amino acid sequence at both termini.

Construction and Expression of Epitope-Tagged GLT-1 Isoforms. To facilitate the study of functional differences and multimerization of GLT-1 isoforms, we produced full-length cDNA constructs with a small epitope tag (V5, HA, or FLAG) in the second extracellular loop. Because well

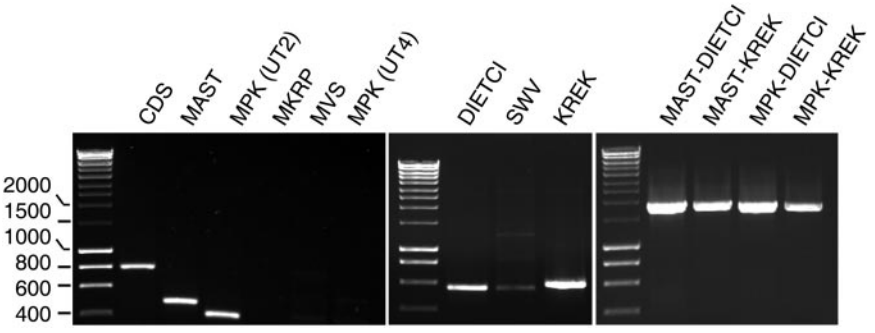

Fig. 1. Identification of N- and C-terminal splice variants of GLT-1 expressed by mouse cerebral cortex. RNA was isolated from mouse cerebral cortex, and RT-PCR was performed using primers against the coding sequence common to all splice variants (CDS) or specific to each N- or C-terminal splice variant. Images are representative of three independent experiments. Transcripts encoding the MAST and MPK(UT2) N-terminal splice variants and the DIETCI and KREK C-terminal splice variants were predominantly expressed, and all four possible full-length isoforms containing combinations of these termini were successfully amplified. PCR products were resolved on a 1% agarose gel against HyperLadder I (Bioline Ltd., London, UK).

characterized antibodies are available to these tags, these extracellular epitopes allow detection of cell-surface GLT-1 and its regulation using a range of experimental techniques that could not be carried out using the commonly available anti-GLT-1 antibodies, all of which bind to intracellular portions of the transporter. In addition, because we are interested in the role of the intracellular N and C termini in mediating GLT-1 function and regulation, we did not wish to produce fusion proteins that might affect these properties. Western blotting analysis was carried out on untagged and tagged MAST-KREK and MPK-DIETCI splice variants expressed in COS-7 cells (Fig. 2). The results show that constructs encoding tagged GLT-1 (Fig. 2, lanes 2–4, 6–8) produce GLT-1-immunoreactive protein with the same banding pattern as untagged GLT-1 (lanes 1 and 5). Under the extraction and electrophoresis conditions used here, we see a predominant immunoreactive band at approximately 75 kDa, and immunoreactive bands of higher molecular weights, similar to the predominant molecular species found in native GLT-1 present in protein extracts of mouse brain (lane 9). The 75-kDa band is always broad, and often appears as a doublet. All the constructs, whether tagged or untagged, produce additional GLT-1-immunoreactive bands of at approximately 53 kDa, which are not found as major species in native GLT-1 in mouse brain extracts. Figure 2, B to D, shows that the tagged isoforms, but not the untagged isoforms or native GLT-1, show specific immunoreactivity when Western blots are probed with anti-epitope antibodies. We note that when probed with anti-HA antibodies or anti-FLAG antibodies, the monomeric forms appear weak, even though they are present as determined by GLT-1 immunoreactivity. This suggests that, in monomeric forms, the HA and FLAG epitopes are partially masked, but because the monomeric form is unchanged in abundance compared with untagged GLT-1 constructs when probed with a GLT-1 antibody (Fig. 2A), the data do not suggest that these epitopes promote multimerization.

A range of cell types (HEK-293, MDCK, and primary mouse astrocytes) were transfected with constructs encoding V5-tagged GLT-1 isoforms. The distribution of GLT-1 was determined by immunofluorescence. Using primary antibodies without cell permeabilization, there is intense cell-surface immunoreactivity for all isoforms. For example, Fig. 3, A to D, shows the expression of V5-tagged MAST-KREK, MAST-DIETCI, MPK-KREK, and MPK-DIETCI at the cell surface of primary mouse astrocytes. Similar expression patterns are observed in all other cell types tested (results not shown). Cell surface expression of GLT-1 constructs was further confirmed using cell-surface biotinylation. A representative experiment using HEK-293 cells stably transfected with V5-MPK-DIETCI is shown in Fig. 3E. The majority of this GLT-1 isoform is biotinylated [i.e., present on the cell surface membrane (M fraction)], and a smaller amount is present in intracellular compartments (IC). This data also shows that although the 75-kDa monomeric form and the higher molecular weight multimeric forms are present on the cell surface, the 53-kDa species is only present in the intracellular fraction.

Functional Studies of GLT-1 Isoforms and Effect of Addition of an Epitope Tag. We next tested whether each GLT-1 isoform is functional (i.e., can support glutamate uptake). Each of the tagged and untagged GLT-1 variants, when transiently transfected in COS-7 cells, supports sodium-dependent uptake of [^{3}H]L-glutamate or [^{3}H]D-aspartate (data not shown). To determine whether GLT-1 isoforms differing in their N and C termini are also functionally different, kinetic analyses were carried out to determine the kinetic parameters of the four main GLT-1 isoforms transiently expressed in COS-7 cells (Table 2). The K_m for L-glutamate uptake does not vary between the four isoforms (range, 43–58 μM). When stably expressed in HEK-293 cells,

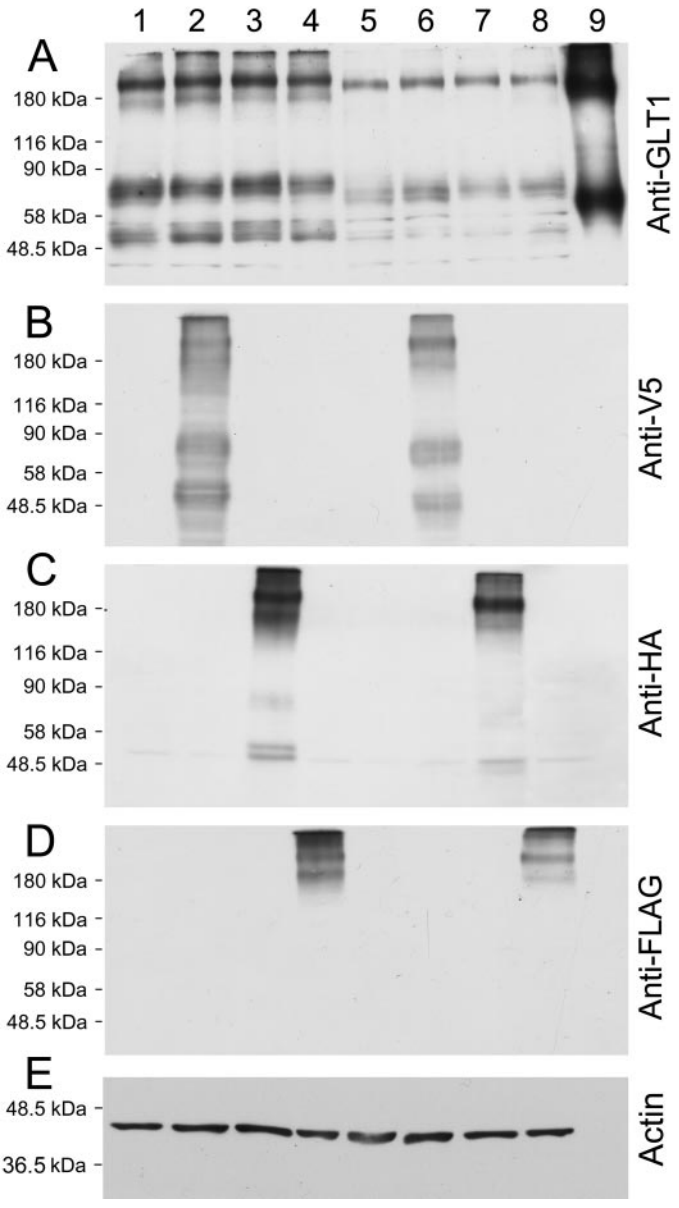

Fig. 2. Western blot analysis of untagged and epitope-tagged GLT-1 splice variants expressed in COS-7 cells. Lysates from transfected COS-7 cells were separated by 9% polyacrylamide gel electrophoresis. Lane 1, transfected with MAST-KREK cDNA; lane 2, V5-MAST-KREK; lane 3, HA-MAST-KREK; lane 4, FLAG-MAST-KREK; lane 5, MPK-DIETCI; lane 6, V5-MPK-DIETCI; lane 7, HA-MPK-DIETCI; lane 8, FLAG-MPK-DIETCI; lane 9, mouse cerebral cortex homogenate. Membranes were probed with B12 anti-GLT-1 antibody (A), anti-V5 (B), anti-HA (C), anti-FLAG (D), and anti-actin (E). Actin bands indicate equivalent loadings of transfected COS-7 cells. The actin band is not visible at this exposure in the cerebral cortex homogenate band because 2 μg of protein was loaded for this sample in contrast to 30 μg from the transfected COS-7 cells.

the K_m values were similar to those obtained using COS-7 cells (data for MPK-DIETCI and V5-tagged MPK-DIETCI shown in Table 2). These data show that the presence of an epitope tag does not alter the affinity of GLT-1 for L-glutamate. We carried out a more detailed analysis of the functional properties of selected isoforms using the two most different GLT-1 isoforms, MAST-KREK and MPK-DIETCI, in stably transfected HEK-293 cells. To determine whether epitope tagging altered the pharmacological properties, we also tested the V5-MPK-DIETCI isoform and, as a control, HEK-293 cells stably transfected with a well characterized inducible rat GLT-1 isoform were also characterized (Dunlop et al., 1999). We determined the IC_{50} values for a wide range of transportable and nontransportable EAAT blockers of different chemical classes (reviewed by Bridges and Esslinger, 2005). Inhibition curves for all 12 compounds on the MAST-KREK GLT-1 isoform are shown in Fig. 4 (nonsubstrate blockers at top, substrate blockers at bottom). These inhibition curves are similar for each of the other three GLT-1 isoforms tested (data not shown). Table 3 shows the IC_{50} values for each of inhibitors against each of the four GLT-1 constructs tested. There is no difference between isoforms in the rank order of potency of the inhibitors or in the IC_{50} values.

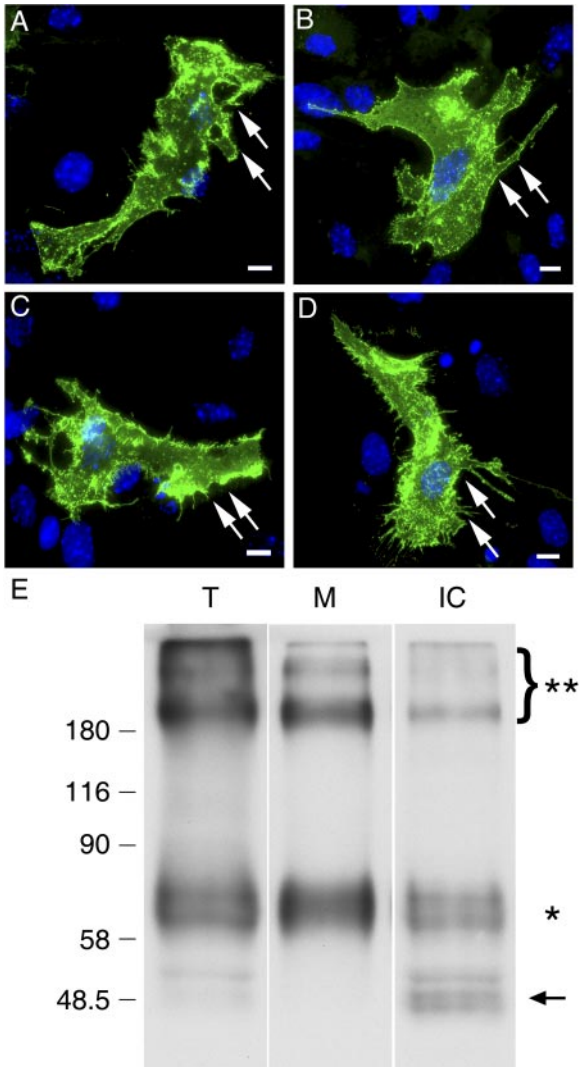

Fig. 3. V5-tagged splice variants of GLT-1 are expressed at the cell surface. Primary mouse cortical astrocytes were grown on glass coverslips and transfected at 17 days in vitro with V5-MAST-KREK (A), V5-MAST-DIETCI (B), V5-MPK-KREK (C), or V5-MPK-DIETCI (D). Immunofluorescence was carried out without permeabilization to allow only V5-immunoreactivity (green) at the cell surface to be detected. Hoescht 33342-stained nuclei are blue. Arrows indicate astrocyte cell boundaries. Scale bar, 10 μm. E, Western blot analysis of total (T), cell surface (M), and intracellular (IC) V5-tagged protein fractions after cell surface protein biotinylation of V5-MPK-DIETCI/HEK-293 cells. Proteins were separated by 9% polyacrylamide gel electrophoresis. Membranes were probed using an antibody against the V5 epitope. **, multimeric forms of GLT-1; *, the glycosylated monomer (~75 kDa). The putative unglycosylated monomer (~53 kDa, not present in the cell surface fraction) is denoted by an arrow. Images are representative of three independent experiments.

TABLE 2
Kinetic properties of GLT-1 variants expressed in cell lines

	K_m	V_{max}
	μM	$pmol \cdot mg^{-1} \cdot min^{-1}$
MAST-KREK	57.9 ± 4.2	1772 ± 319
MAST-DIETCI	58.5 ± 4.4	2295 ± 370
MPK-KREK	42.8 ± 4.8	1033 ± 197
MPK-DIETCI	46.6 ± 4.1	824 ± 191
MPK-DIETCI (HEK-293)	46.5 ± 5.9	4409 ± 641
V5-MPK-DIETCI (HEK293)	48.0 ± 3.4	3849 ± 108

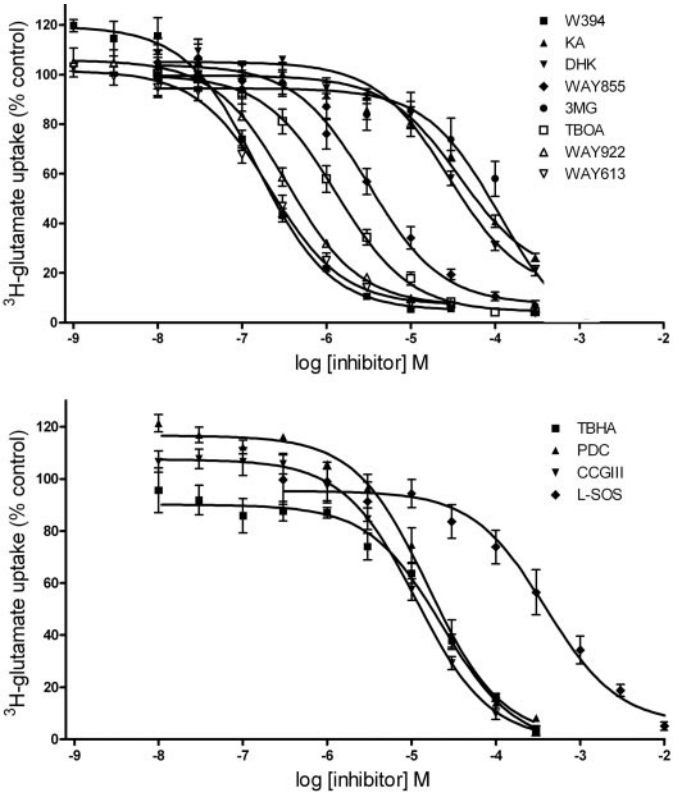

Fig. 4. Concentration response curves for L-glutamate transporter inhibition. Twelve EAAT inhibitors were tested for their ability to block [^{3}H]L-glutamate uptake into HEK-293 cells stably expressing the MAST-KREK isoform of GLT-1. Top, the nonsubstrate inhibitors WAY-213394 (W-394), WAY-213613 (WAY-613), WAY-212922 (WAY-922), DL-*threo*-β-benzyloxyaspartate (TBOA), WAY-144855 (WAY-855), dihydrokainate (DHK), kainite (KA), and (±)-*threo*-3-methylglutamate (3MG). Bottom, the substrate inhibitors *threo*-β-hydroxyaspartate (TBHA), L-transpyrrolidine-2,4-dicarboxylic acid (PDC), 2*S*,1′*S*,2′*R*-2-(carboxycyclopropyl)glycine (CCGIII), and L-serine-*O*-sulfate (L-SOS). Data are presented as percentage of maximum Na^+-dependent uptake in the absence of inhibitor. Data are mean ± S.E.M. from between three and five independent experiments.

Homomeric and Heteromeric Association of GLT-1 Isoforms. To determine whether any of the GLT-1 isoforms has a dominant-negative effect on expression, we expressed every combination of the four isoforms in a pair-wise fashion, using both V5- and HA-tagged forms to enable detection using dual color immunofluorescence on unpermeabilized cells. For each of the 10 possible pairs, both the HA- and the V5- tagged isoforms were expressed on the cell surface with a complete overlap in distribution (Fig. 5).

To determine whether GLT-1 isoforms can form homomers and/or heteromers, coimmunoprecipitation experiments were carried out using HEK-293 cells transfected with each of the pair-wise combinations of HA- and V5-tagged GLT-1 isoforms. Figure 6 shows examples of blots for two of the cotransfected pairs (Supplemental Figs. 1 and 2 shows blots for all the pair-wise combinations). Detergent-solubilized cell extracts from transiently transfected cultures with abundant coexpression of HA- and V5-tagged GLT-1 (V5- and HA-immunoreactivity of extracts shown in Fig. 6A) were incubated with anti-V5 antibody (+) to precipitate V5-immunoreactive species or an IgG_{2A} control antibody (−) as a negative control. As an additional control to eliminate the possibility that multimers were forming during the experimental procedure, extracts from cells singly transfected with V5-MAST-KREK GLT-1 and HA-MAST-DIETCI GLT-1 were mixed together. After immunoprecipitation with protein A/G agarose, immunoprecipitates were analyzed by Western blot, using either an anti-V5 antibody (Fig. 6B, left) or an anti-HA antibody (Fig. 6B, right). As expected, V5 immune pellets display good anti-V5 immunoreactivity, with bands present representing the monomeric and higher molecular weight species present. The anti-HA blot reveals a strongly immunoreactive band of high molecular weight only in the samples that originate from cells that coexpress V5- and HA-tagged GLT-1 and where the anti-V5 antibody is used for immunoprecipitation. This prominent band is consistent with a multimeric form of GLT-1 containing both of the transfected isoforms and is found in each of the combinations of GLT-1 isoforms tested but none of the negative controls.

An additional technique was used to confirm whether GLT-1 variants can associate. Pair-wise combinations of HA- and FLAG-tagged GLT-1 isoforms were transfected into HEK-293 cells. As a positive control, cells cotransfected with HA- and FLAG-tagged histamine H_4 receptor subunits were used because the H_4 receptor has previously been shown to form multimers (van Rijn et al., 2006). Whole cells were suspended and subjected to tr-FRET using Eu^{3+}-labeled anti-FLAG as the donor fluorophore and XL-665-labeled anti-HA as the acceptor fluorophore. As a negative control, for each pair, cells expressing each one of the GLT-1 isoforms were mixed; in these samples, any tr-FRET signal cannot be due to the presence of GLT-1 multimers. These FRET studies (Fig. 6C) reveal that each of the pair-wise combinations of GLT-1 isoforms, when coexpressed, produces a strong tr-FRET signal, indicating close spatial proximity of the HA and V5 tags. On the other hand, mixed cells do not produce a tr-FRET signal. The difference between cotransfected and pooled cells is highly significant ($p < 0.0001$).

Regulation of Cell Surface GLT-1 by Phorbol Ester. Activation of protein kinase C (PKC) by phorbol esters has been suggested to drive an internalization of GLT-1 in a number of cell types, including stably and transiently transfected C6 glioma, primary mouse astrocytes induced to express GLT-1 by dibutyryl cAMP, and neuron-enriched rat cortical cocultures (Susarla and Robinson 2008; Zhou and Sutherland 2004; Kalandadze et al., 2002; González et al., 2005; Guillet et al., 2005). As a proof of concept to test the utility of these novel epitope-tagged GLT-1 isoforms to study regulated trafficking, we used HEK-293 cells stably expressing V5-MPK-DIETCI and surveyed the cell surface and intracellular expression of GLT-1 using an anti-V5 antibody. The extracellular epitope allows consecutive staining of extracellular and intracellular immunoreactivity. Figure 7, A and B, shows immunofluorescent images that reveal the redistribution of V5-immunoreactivity from the cell surface membrane (green) to intracellular compartments (red) within 1 h of exposure to phorbol ester (100 nM). Cell surface biotinylation was also carried out (Fig. 7C), and the data were quantified (Fig. 7, D and E). Treatment with PMA results in a loss of V5-MPK-DIETCI from the cell surface and a corresponding increase in the intracellular compartment. This effect is maximal at 30 min, resulting in a 31.6% loss of V5-MPK-DIETCI from the cell surface (membrane normalized band intensities: control, 0.76 ± 0.04; after 30-min PMA treatment, 0.52 ± 0.03; intracellular normalized band intensities: control, 0.24 ± 0.04; after 30-min PMA treatment, 0.48 ± 0.03). A significant (25%) loss of total V5-immunoreactivity was also observed (Fig. 7D) (normalized band intensities: control, 29.6 ± 1.0; 60-min PMA, 22.2 ± 1.6), suggesting that GLT-1 is degraded after activation of PKC.

TABLE 3

Inhibition of GLT-1 variants by a range of uptake blockers

Values are means ± S.E.M. derived from at least three independent experiments. The rank order and actual IC_{50} values for this series of inhibitors do not differ among the cell lines tested ($P < 0.01$).

	irGLT-1	MAST-KREK	MPK-DIETCI	V5-MPK-DIETCI
WAY-213394	106.3 ± 28.4 nM	87.8 ± 4.2 nM	119.2 ± 26.4 nM	152.7 ± 8.8 nM
WAY-213613	182.7 ± 32.9 nM	152.0 ± 36.6 nM	225.6 ± 34.5 nM	220.6 ± 41.2 nM
WAY-212922	200.3 ± 42.0 nM	177.3 ± 34.0 nM	252.0 ± 19.0 nM	355.6 ± 70.4 nM
TBOA	1.9 ± 0.5 μM	1.7 ± 0.2 μM	2.2 ± 0.5 μM	1.3 ± 0.1 μM
WAY-144855	2.4 ± 0.5 μM	1.5 ± 0.2 μM	3.1 ± 0.3 μM	3.3 ± 0.6 μM
CCGIII	6.3 ± 1.1 μM	5.6 ± 2.6 μM	9.7 ± 2.3 μM	11.4 ± 1.4 μM
PDC	11.1 ± 2.2 μM	11.0 ± 1.6 μM	10.4 ± 2.0 μM	17.2 ± 5.4 μM
TβHA	19.0 ± 5.3 μM	12.8 ± 4.7 μM	24.9 ± 4.9 μM	22.8 ± 4.7 μM
DHK	42.6 ± 20.7 μM	39.1 ± 21.5 μM	41.3 ± 9.1 μM	28.2 ± 5.3 μM
KA	92.4 ± 65.8 μM	76.2 ± 37.5 μM	51.2 ± 13.8 μM	38.0 ± 5.1 μM
3MG	115.2 ± 17.5 μM	92.1 ± 32.0 μM	93.7 ± 16.1 μM	108.5 ± 23.4 μM
L-SOS	207.8 ± 21.7 μM	232.7 ± 33.4 μM	400.6 ± 58.1 μM	452.1 ± 159.9 μM

TBOA, DL-*threo*-β-benzyloxyaspartate; CCGIII, 2*S*,1′*S*,2′*R*-2-(carboxycyclopropyl)glycine; PDC, L-transpyrrolidine-2,4-dicarboxylic acid; TβHA, *threo*-β-hydroxyaspartate; DHK, dihydrokainate; KA, kainite; 3MG, (±)-*threo*-3-methylglutamate; L-SOS, L-serine-*O*-sulfate.

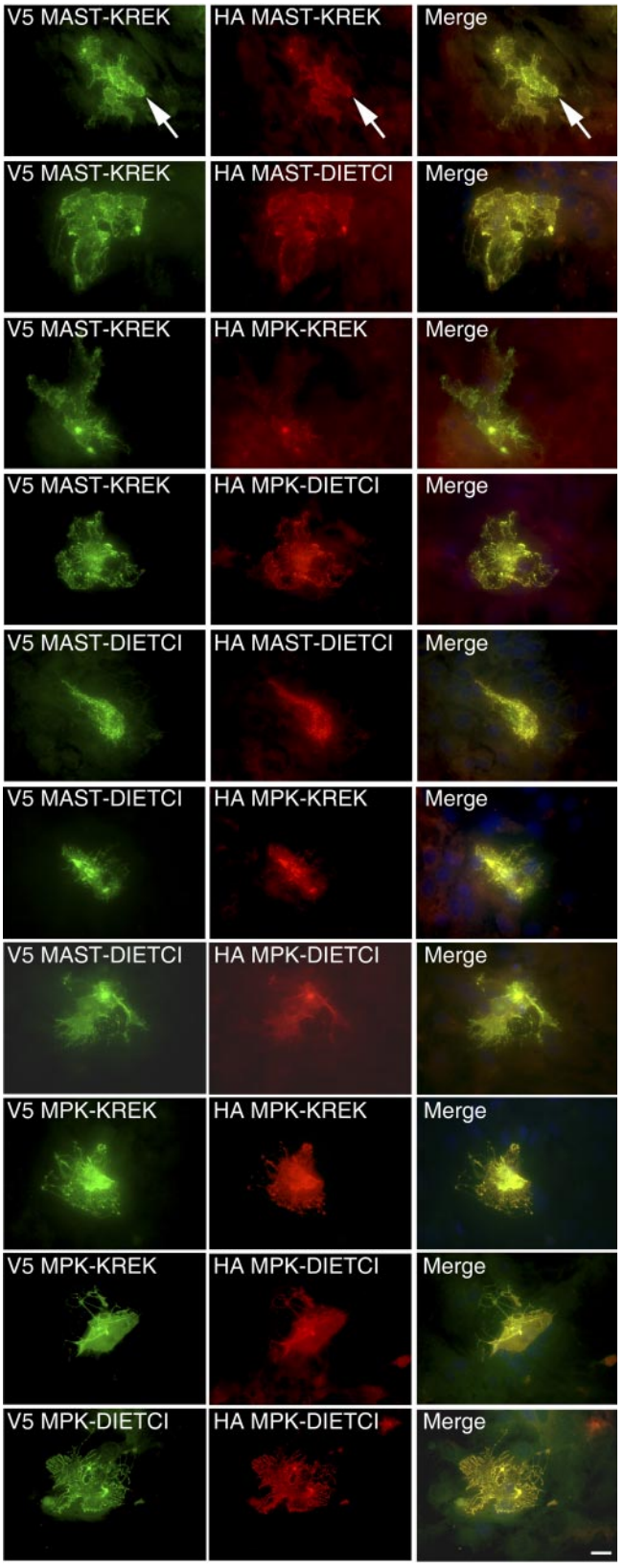

Fig. 5. Immunofluorescence micrographs showing colocalization of GLT-1 splice variants at the cell surface of primary astrocytes. Primary astrocytes were cotransfected with pairs of GLT-1 splice variants (one containing the V5 epitope tag, one containing the HA epitope tag). V5 immunofluorescence of unpermeabilized cells is shown in green; HA immunofluorescence is shown in red. The merged color image is shown on the right hand side. Arrows in the first row indicate cell boundaries of astrocytes. Images are representative of nine fields captured. Scale bars, 10 μm.

In addition, disease-producing SOD1 mutants that down-regulate GLT-1 in transgenic mice (e.g., Bendotti et al., 2001) or in cultured cells (e.g., Tortarolo et al., 2004) caused a marked decrease in cell surface expression of GLT-1 in primary astrocytes cotransfected with V5-tagged GLT-1 and green fluorescent protein N-terminal fusion proteins with different human superoxide dismutase-1 (SOD1) mutants: GFP-hSOD1^{wt}, GFP-hSOD1^{G93A}, GFP-hSOD1^{A4V}, GFP-

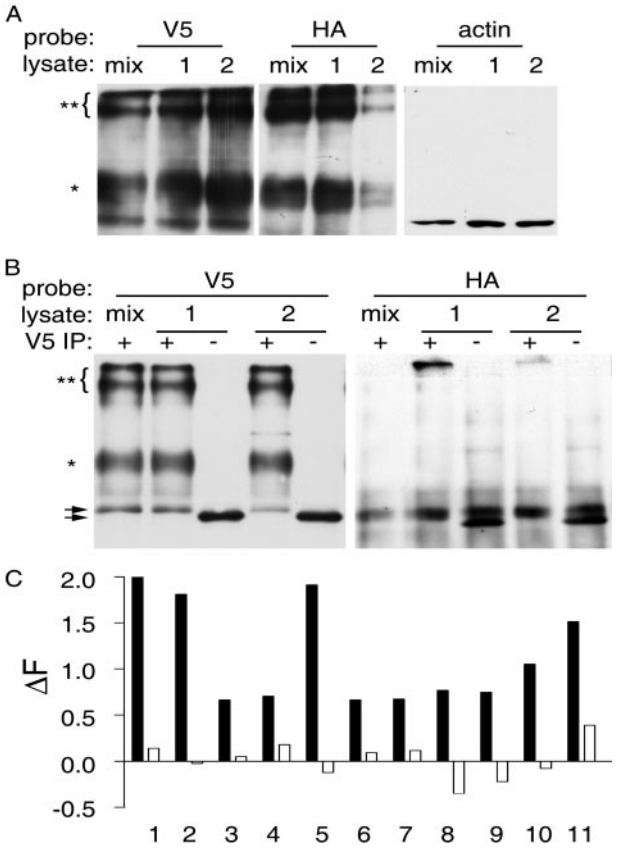

Fig. 6. Coimmunoprecipitation and tr-FRET show that GLT-1 isoforms can form homomers and heteromers. A, Western blot analysis of V5-, HA-, and actin-immunoreactivity of solubilized extracts before the immunoprecipitation procedure: mix, extracts from HEK-293 cells transfected with V5-MAST-KREK mixed with extracts from HEK-293 cells transfected with HA-MAST-DIETCI; 1, extracts from HEK-293 cells cotransfected with V5-MAST-KREK and HA-MAST-DIETCI; 2, extracts from HEK-293 cells cotransfected with V5-MAST-KREK and HA-MPK-KREK. *, monomeric GLT-1; **, multimeric forms of GLT-1. Actin blot shows equivalent amounts of mixed and cotranfected samples were used for immunoprecipitation (B). After coimmunoprecipitation, the V5- and HA-immunoreactivity of the immune pellets were analyzed by Western blot: mix, 1, and 2 as described for A. +, anti-V5 immune pellet; −, IgG_{2A} immune pellet. Arrows at left indicate bands resulting from antibody heavy chains. C, the homo- and heteromultimerization of GLT-1 isoforms was evaluated with tr-FRET. The change in fluorescent signal over background (ΔF) was calculated for all combinations of splice variant pairs. Assays were performed using cells coexpressing pairs of epitope-tagged splice variants (or H_4Rs) (filled bars) or cells pooled from separate transfections with individual epitope-tagged splice variants (or H_4Rs) (open bars). Pair 1, FLAG-MAST-KREK + HA-MAST-KREK; pair 2, FLAG-MAST-KREK + HA-MAST-DIETCI; pair 3, FLAG-MAST-KREK + HA-MPK-KREK; pair 4, FLAG-MAST-KREK + HA-MPK-DIETCI; pair 5, FLAG-MAST-DIETCI + HA-MAST-DIETCI; pair 6, FLAG-MAST-DIETCI + HA-MPK-KREK; pair 7, FLAG-MAST-DIETCI + HA-MPK-DIETCI; pair 8, FLAG-MPK-KREK + HA-MPK-KREK; pair 9, FLAG-MPK-KREK + HA-MPK-DIETCI; pair 10, FLAG-MPK-DIETCI + HA-MPK-DIETCI; pair 11, FLAG-H_4R + HA-H_4R. One representative experiment is shown in this figure.

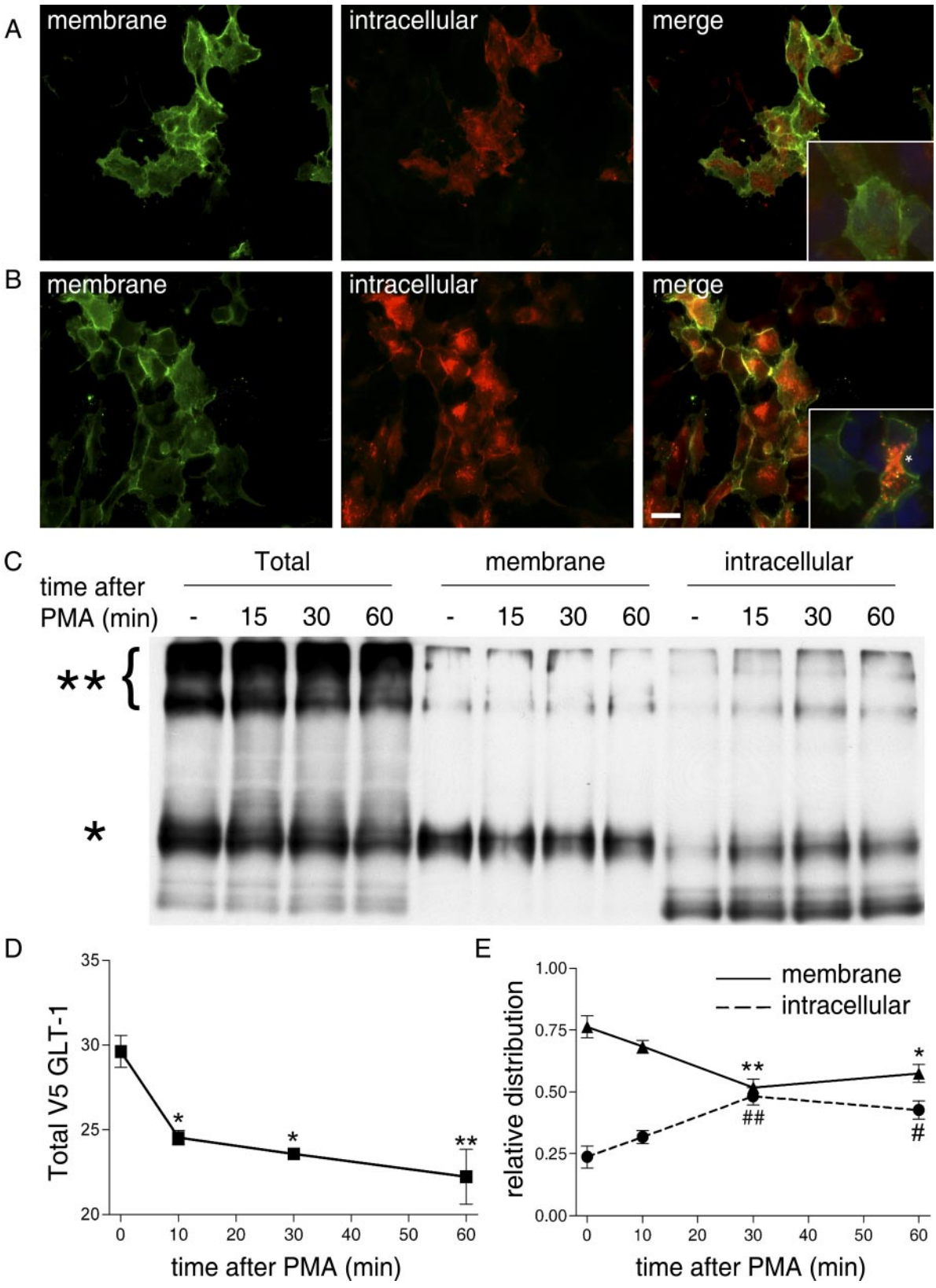

Fig. 7. Cell surface GLT-1 is regulated by phorbol ester. Immunofluorescence micrographs (representative of between three and seven fields captured) of V5-MPK-DIETCI/HEK-293 cells for control (A) and treated with 100 nM PMA for 60 min (B). For each set of images, cell surface expression of V5 epitope (green) is on the left, intracellular expression of V5 epitope (red) is in the middle, and the merged color image is on the right. Scale bars, 20 μm. In A and B, insets picture individual cells at higher magnifications, to show internalization of tagged GLT-1 isoform after phorbol ester treatment. C, V5-MPK-DIETCI/HEK-293 cells were treated with 100 nM PMA for 0 to 60 min, followed by cell surface protein biotinylation to separate the cell surface and intracellular protein fractions. Fractions were analyzed by Western blot (representative film shown). Proteins were separated by 9% polyacrylamide gel electrophoresis and membranes were probed for the V5 epitope. *, monomeric GLT-1; **, multimeric forms of GLT-1. D, quantification of total lysate band intensities. E, quantification of relative distribution of cell surface and intracellular V5. The sum of the monomeric and multimeric bands was used for quantification. Data are presented as mean normalized band intensity ± S.E.M. from three independent experiments, consisting of duplicates of each condition. *, $p < 0.05$; **, $p < 0.01$; #, $p < 0.05$; ##, $p < 0.01$ compared with zero time control using one-way ANOVA with the Bonferroni post hoc test.

hSOD1^{G37R}, GFP-hSOD1^{G85R} (De Vos et al., 2007; Supplementary Fig. 3).

Discussion

Using RT-PCR, full-length mRNAs encoding 4 of the 12 possible isoforms are found to be expressed at detectable levels. These transcripts encode MAST or MPK N termini with either the DIETCI or KREK C termini. Because previous reports have only focused on either the N or the C termini, this is the first analysis to identify the most important full-length GLT-1 isoforms that have the potential to be expressed in the CNS. A quantification of relative abundance of the full-length transcripts (approximately 1.7 kilobase pairs) could not be carried out because of the technical difficulties of such an approach. Real-time PCR is precluded because of the amplicon length (Nolan et al., 2006). Although relative and absolute quantification of transcript abundance was not carried out here, we note that the MAST-KREK form and the MPK-DIETCI isoform are the most and least abundant, respectively, of the four isoforms found (results not shown). The relative abundance of the C-terminal (SWV, DIETCI, KREK) and N-terminal portions of GLT-1 (MAST, MPK) shown qualitatively here are in close agreement with previously published studies (Münch et al., 2002; Lauriat et al., 2006). The failure to detect the MKRP N terminus in this study could represent a lack of expression in mouse, because this variant has only been amplified from rat astrocyte cultures (Rozyczka and Engele, 2005).

We generated GLT-1 variants with a small epitope tag in the second extracellular loop and carried out a detailed characterization of the molecular and pharmacological properties of these novel constructs. Glutamate transporters are generally accepted to form multimers, with evidence from X-ray crystallography, electron microscopy, chemical cross-linking, and blue-native polyacrylamide gel electrophoresis predominantly indicating a trimeric quaternary structure. (Danbolt et al., 1992; Haugeto et al., 1996; Gendreau et al., 2004; Yernool et al., 2004; Raunser et al., 2005). Using Western blotting, we observed that each of the four isoforms, whether tagged or not, showed a predominant broad band of molecular weight of approximately 75 kDa, which sometimes appears as a doublet, corresponding to the monomer. The presence of a range of bands of approximately this size may be due to variations in post-translational modification and/or proteolysis of GLT-1 (Danbolt 2001; Boston-Howes et al., 2006; Gibb et al., 2007). As well as monomeric GLT-1, all constructs and endogenous GLT-1 show a cluster of immunoreactive bands with molecular masses of >180 kDa. On the basis of the band sizes on Western blots, our data suggest that trimers are the main multimeric species, but the data do not rule out higher order assemblies. We note that these higher molecular mass species are retained even during electrophoresis in denaturing conditions, and therefore the multimers observed by Western blotting are likely to represent oligomeric species that are stabilized by covalent linkages that occur during tissue processing.

For the tagged variants, in some cases the signal from the monomeric forms is weak, suggesting that in the monomeric forms, the epitope is partially masked under these conditions. All the constructs, tagged or untagged, produce additional immunoreactive bands at approximately 53 kDa that are not found in endogenous GLT-1. Cell surface biotinylation shows this species is intracellular. We believe this represents unglycosylated immature GLT-1 that is present in intracellular compartments (e.g., Raunser et al., 2005).

Cell-surface biotinylation, immunofluorescence and glutamate uptake assays show that all four GLT-1 isoforms tested reach the cell surface in a functional state. The majority of monomeric and multimeric GLT-1 are present on the cell surface, with a smaller amount present in intracellular compartments. The K_m values obtained (range, 43–58 μM) show that each isoform has similar affinity for L-glutamate and is likely to operate over the same range of glutamate concentrations. The K_m values are in good agreement with published values of between 10 and 100 μM for heterologous GLT-1 expression in cell lines (Arriza et al., 1994; Dunlop et al., 1999; Danbolt, 2001) and native GLT-1 (Bridges and Esslinger, 2005). The V_{max} varies between isoforms with the expression levels of the protein as assessed by Western blotting (results not shown). Thus differences in V_{max} between isoforms reflect different transfection or translation efficiencies rather than inherent differences in glutamate transport kinetics. The similarity between isoforms was reflected by identical absolute and rank order of potency of a range of glutamate transport inhibitors. Therefore, pharmacological analysis shows no differences between the main GLT-1 isoforms. The data show that addition of an epitope tag into the second extracellular loop of GLT-1 does not affect functional properties; therefore, epitope-tagged GLT-1 can be used as a novel tool.

Whether GLT-1 isoforms can form heteromers as well as homomers had not previously been determined. Coimmunoprecipitation experiments using HEK-293 cells transfected with each pairwise combination of HA- and V5-tagged GLT-1 isoforms show the presence of HA- and V5-positive bands corresponding to multimeric assemblies. The band size is consistent with GLT-1 trimers and is found in each combination of GLT-1 isoforms but not negative controls. tr-FRET was also used and revealed that each of the pair-wise combinations of GLT-1 isoforms, when coexpressed but not when mixed, produced a signal indicating close spatial proximity of HA and V5 tags. Both sets of data show, for the first time, that GLT-1 subunits can directly associate with one another to form homomers and heteromers that are expressed on the cell surface.

These data together strongly suggest that the high molecular weight GLT-1 species found on Western blots are not simply artifacts due to processing or oxidative multimerization (e.g., Trotti et al., 1998) but are genuine multimeric assemblies present on the cell surface of living cells. The exact stoichiometry of the GLT-1 multimers on the cell surface, and the proportion of GLT-1 that is assembled into oligomers, is not known.

The four GLT-1 isoforms could combine in many permutations to form numerous different multimers. When expressed alone, each of the four main GLT-1 isoforms appears to have identical functional properties, discussed above. Although we did not directly test every isoform combination, we consider it unlikely, based on these results, that heteromeric combinations of GLT-1 isoforms would have any differences in their activities or sensitivity to inhibitors compared with homomeric assemblies. It is possible that certain GLT-1 isoforms act in a dominant-

negative manner, to reduce glutamate transporter activity. For example, an intron-7 retention splice variant has been suggested to act in this manner (Lin et al., 1998), and a splice variant of a related transporter, GLAST, reduces insertion of the wild-type protein into the plasma membrane (Vallejo-Illarramendi et al., 2005). To examine this possibility directly, we expressed every combination of the four isoforms in a pair-wise fashion and showed membrane localization of GLT-1 is unaffected by the expression of a second GLT-1 isoform. We exclude the possibility that any of the four N- and C-terminal GLT-1 isoforms can block cell-surface expression of other GLT-1 isoforms.

Functional differences between GLT-1 homomers and heteromers made up of the four different N- and C-terminal isoforms remain elusive, and none has been discovered in this study. We speculate that the different multimeric assemblies may represent pools of GLT-1 that can be differentially regulated under physiological or pathophysiological situations. For example, multimers containing certain GLT-1 isoforms may be relatively more stable at the cell membrane than others, because of differences in N- and C-terminal amino acid sequences. For example, the DIETCI but not the KREK C terminus of GLT-1 contains a PICK1 postsynaptic density 95/discs large/zona occludens binding motif that influences the ability of GLT-1 to be trafficked from the plasma membrane (Bassan et al., 2008). GLT-1 variants with the DIETCI C terminus also bind postsynaptic density 95 (González-González et al., 2008). Further studies are under way to test these points.

Our novel epitope-tagged constructs are a useful tool to study GLT-1 regulation at the cell surface under physiological and pathophysiological stimulation. Activation of PKC by phorbol esters has been shown previously to drive an internalization of GLT-1 in several cell types (e.g., Kalandadze et al., 2002; Susarla and Robinson, 2008). Our immunofluorescence data support this concept qualitatively, and cell-surface protein biotinylation data from HEK-293 cells expressing these novel constructs confirm that PMA results in a loss of cell-surface V5-MPK-DIETCI and a corresponding increase in intracellular protein. The 32% loss of V5-MPK-DIETCI from the cell surface after 30-min treatment with 100 nM PMA closely agrees with previous results in a different system (Kalandadze et al., 2002). The decrease from the plasma membrane, and the relevant aspects of internalization, intracellular pools, and re-insertion (Beart and O'Shea, 2007), along with the regulation of different GLT-1 variants, should be the subject of further studies. GLT-1 down-regulation occurs in patients with ALS (Rothstein et al., 1995) and is considered to be a disease-modifying event in motor neuron degeneration in ALS (Rattray and Bendotti, 2006; Beart and O'Shea, 2007). The down-regulation of GLT-1 is a highly selective phenomenon in astrocytes expressing disease-relevant SOD1 mutants, because a related glutamate transporter, GLAST, is not down-regulated (Tortarolo et al., 2004). Here we show proof-of-concept data that V5-tagged GLT-1 is removed from the membrane of primary astrocytes after coexpression of SOD1 mutants that cause ALS. Thus the novel epitope-tagged GLT-1 constructs will allow more detailed study of pathophysiological regulation of GLT-1 and its variants.

Acknowledgments

We thank Angela Kramer and Zhuangwei Lou for expert technical support in helping prepare the stably expressing HEK-293 cell lines. Because of space limitations, some important articles were not referenced.

References

Arriza JL, Fairman WA, Wadiche JI, Murdoch GH, Kavanaugh MP, and Amara SG (1994) Functional comparisons of three glutamate transporter subtypes cloned from human motor cortex. *J Neurosci* **14:**5559–5569.

Bassan M, Liu H, Madsen KL, Armsen W, Zhou J, Desilva T, Chen W, Paradise A, Brasch MA, Staudinger J, et al. (2008) Interaction between the glutamate transporter GLT1b and the synaptic PDZ domain protein PICK1. *Eur J Neurosci* **27:**66–82.

Beart PM and O'Shea RD (2007) Transporters for L-glutamate: an update on their molecular pharmacology and pathological involvement. *Br J Pharmacol* **150:**5–17.

Bendotti C, Tortarolo M, Suchak SK, Calvaresi N, Carvelli L, Bastone A, Rizzi M, Rattray M, and Mennini T (2001) Transgenic SOD1 G93A mice develop reduced GLT-1 in spinal cord without alterations in cerebrospinal fluid glutamate levels. *J Neurochem* **79:**737–746.

Boston-Howes W, Gibb SL, Williams EO, Pasinelli P, Brown RH Jr, and Trotti D (2006) Caspase-3 cleaves and inactivates the glutamate transporter EAAT2. *J Biol Chem* **281:**14076–14084.

Bridges RJ and Esslinger CS (2005) The excitatory amino acid transporters: pharmacological insights on substrate and inhibitor specificity of the EAAT subtypes. *Pharmacol Ther* **107:**271–285.

Chen W, Aoki C, Mahadomrongkul V, Gruber CE, Wang GJ, Blitzblau R, Irwin N, and Rosenberg PA (2002) Expression of a variant form of the glutamate transporter GLT1 in neuronal cultures and in neurons and astrocytes in the rat brain. *J Neurosci* **22:**2142–2152.

Danbolt NC, Storm-Mathisen J, and Kanner BI (1992) An [Na^+ + K^+]coupled L-glutamate transporter purified from rat brain is located in glial cell processes. *Neuroscience* **51:**295–310.

Danbolt NC (2001) Glutamate uptake. *Prog Neurobiol* **65:**1–105.

De Vos KJ, Chapman AL, Tennant ME, Manser C, Tudor EL, Lau KF, Brownlees J, Ackerley S, Shaw PJ, McLoughlin DM, et al. (2007) Familial amyotrophic lateral sclerosis-linked SOD1 mutants perturb fast axonal transport to reduce axonal mitochondria content. *Hum Mol Genet* **16:**2720–2728.

Dunlop J, Lou Z, Zhang Y, and McIlvain HB (1999) Inducible expression and pharmacology of the human excitatory amino acid transporter 2 subtype of L-glutamate transporter. *Br J Pharmacol* **128:**1485–1490.

Dunlop J, McIlvain HB, Carrick TA, Jow B, Lu Q, Kowal D, Lin S, Greenfield A, Grosanu C, Fan K, et al. (2005) Characterization of novel aryl-ether, biaryl, and fluorene aspartic acid and diaminopropionic acid analogs as potent inhibitors of the high-affinity glutamate transporter EAAT2. *Mol Pharmacol* **68:**974–982.

Gendreau S, Voswinkel S, Torres-Salazar D, Lang N, Heidtmann H, Detro-Dassen S, Schmalzing G, Hidalgo P, and Fahlke C (2004) A trimeric quaternary structure is conserved in bacterial and human glutamate transporters. *J Biol Chem* **279:**39505–39512.

Gibb SL, Boston-Howes W, Lavina ZS, Gustincich S, Brown RH Jr, Pasinelli P, and Trotti D (2007) A caspase-3-cleaved fragment of the glial glutamate transporter EAAT2 is sumoylated and targeted to promyelocytic leukemia nuclear bodies in mutant SOD1-linked amyotrophic lateral sclerosis. *J Biol Chem* **282:**32480–32490.

González-González IM, García-Tardón N, Cubelos B, Giménez C, and Zafra F (2008) The glutamate transporter GLT1b interacts with the scaffold protein PSD-95. *J Neurochem* **105:**1834–1848.

González MI, Susarla BT, and Robinson MB (2005) Evidence that protein kinase calpha interacts with and regulates the glial glutamate transporter GLT-1. *J Neurochem* **94:**1180–1188.

Guillet BA, Velly LJ, Canolle B, Masmejean FM, Nieoullon AL, and Pisano P (2005) Differential regulation by protein kinases of activity and cell surface expression of glutamate transporters in neuron-enriched cultures. *Neurochem Int* **46:**337–346.

Haugeto O, Ullensvang K, Levy LM, Chaudhry FA, Honoré T, Nielsen M, Lehre KP, and Danbolt NC (1996) Brain glutamate transporter proteins form homomultimers. *J Biol Chem* **271:**27715–27722.

Kalandadze A, Wu Y, and Robinson MB (2002) Protein kinase c activation decreases cell surface expression of the GLT-1 subtype of glutamate transporter. Requirement of a carboxyl-terminal domain and partial dependence on serine 486. *J Biol Chem* **277:**45741–45750.

Lauriat TL, Dracheva S, Chin B, Schmeidler J, McInnes LA, and Haroutunian V (2006) Quantitative analysis of glutamate transporter MRNA expression in prefrontal and primary visual cortex in normal and schizophrenic brain. *Neuroscience* **137:**843–851.

Lin CL, Bristol LA, Jin L, Dykes-Hoberg M, Crawford T, Clawson L, and Rothstein JD (1998) Aberrant RNA processing in a neurodegenerative disease: the cause for absent EAAT2, a glutamate transporter, in amyotrophic lateral sclerosis. *Neuron* **20:**589–602.

Münch C, Ebstein M, Seefried U, Zhu B, Stamm S, Landwehrmeyer GB, Ludolph AC, Schwalenstöcker B, and Meyer T (2002) Alternative splicing of the 5′-sequences of the mouse EAAT2 glutamate transporter and expression in a transgenic model for amyotrophic lateral sclerosis. *J Neurochem* **82:**594–603.

Nolan T, Hands RE, and Bustin SA (2006) Quantification of MRNA using real-time RT-PCR. *Nat Protoc* **1:**1559–1582.

Pines G, Danbolt NC, Bjørås M, Zhang Y, Bendahan A, Eide L, Koepsell H, Storm-Mathisen J, Seeberg E, and Kanner BI (1992) Cloning and expression of a rat brain L-glutamate transporter. *Nature* **360:**464–467.

Pollard M and McGivan J (2000) The rat hepatoma cell line H4-II-E-C3 expresses

high activities of the high-affinity glutamate transporter GLT-1A. *FEBS Lett* **484:**74–76.
Pow DV, Naidoo T, Lingwood BE, Healy GN, Williams SM, Sullivan RK, O'Driscoll S, and Colditz PB (2004) Loss of glial glutamate transporters and induction of neuronal expression of GLT-1B in the hypoxic neonatal pig brain. *Brain Res Dev Brain Res* **153:**1–11.
Rattray M and Bendotti C (2006) Does excitotoxic cell death of motor neurons in ALS arise from glutamate transporter and glutamate receptor abnormalities? *Exp Neurol* **201:**15–23.
Rauen T, Wiessner M, Sullivan R, Lee A, and Pow DV (2004) A new GLT1 splice variant: cloning and immunolocalization of GLT1c in the mammalian retina and brain. *Neurochem Int* **45:**1095–1106.
Raunser S, Haase W, Bostina M, Parcej DN, and Kühlbrandt W (2005) High-yield expression, reconstitution and structure of the recombinant, fully functional glutamate transporter GLT-1 from rattus norvegicus. *J Mol Biol* **351:**598–613.
Rothstein JD, Martin L, Levey AI, Dykes-Hoberg M, Jin L, Wu D, Nash N, and Kuncl RW (1994) Localization of neuronal and glial glutamate transporters. *Neuron* **13:**713–725.
Rothstein JD, Van Kammen M, Levey AI, Martin LJ, and Kuncl RW (1995) Selective loss of glial glutamate transporter GLT-1 in amyotrophic lateral sclerosis. *Ann Neurol* **38:**73–84.
Rozyczka J and Engele J (2005) Multiple 5′-splice variants of the rat glutamate transporter-1. *Brain Res Mol Brain Res* **133:**157–161.
Schmitt A, Asan E, Lesch KP, and Kugler P (2002) A splice variant of glutamate transporter GLT1/EAAT2 expressed in neurons: cloning and localization in rat nervous system. *Neuroscience* **109:**45–61.
Sullivan R, Rauen T, Fischer F, Wiessner M, Grewer C, Bicho A, and Pow DV (2004) Cloning, transport properties, and differential localization of two splice variants of GLT-1 in the rat CNS: implications for CNS glutamate homeostasis. *Glia* **45:**155–169.
Susarla BT and Robinson MB (2008) Internalization and degradation of the glutamate transporter GLT-1 in response to phorbol ester. *Neurochem Int* **52:**709–722.
Tanaka K, Watase K, Manabe T, Yamada K, Watanabe M, Takahashi K, Iwama H, Nishikawa T, Ichihara N, Kikuchi T, et al. (1997) Epilepsy and exacerbation of brain injury in mice lacking the glutamate transporter GLT-1. *Science* **276:**1699–1702.
Tortarolo M, Crossthwaite AJ, Conforti L, Spencer JP, Williams RJ, Bendotti C, and Rattray M (2004) Expression of SOD1 G93A or wild-type SOD1 in primary cultures of astrocytes down-regulates the glutamate transporter GLT-1: lack of involvement of oxidative stress. *J Neurochem* **88:**481–493.
Trotti D, Danbolt NC, and Volterra A (1998) Glutamate transporters are oxidant-vulnerable: a molecular link between oxidative and excitotoxic neurodegeneration? *Trends Pharmacol Sci* **19:**328–334.
Utsunomiya-Tate N, Endou H, and Kanai Y (1997) Tissue specific variants of glutamate transporter GLT-1. *FEBS Lett* **416:**312–316.
Vallejo-Illarramendi A, Domercq M, and Matute C (2005) A novel alternative splicing form of excitatory amino acid transporter 1 is a negative regulator of glutamate uptake. *J Neurochem* **95:**341–348.
van Rijn RM, Chazot PL, Shenton FC, Sansuk K, Bakker RA, and Leurs R (2006) Oligomerization of recombinant and endogenously expressed human histamine H(4) receptors. *Mol Pharmacol* **70:**604–615.
Yernool D, Boudker O, Jin Y, and Gouaux E (2004) Structure of a glutamate transporter homologue from pyrococcus horikoshii. *Nature* **431:**811–818.
Yi JH, Pow DV, and Hazell AS (2005) Early loss of the glutamate transporter splice-variant GLT-1v in rat cerebral cortex following lateral fluid-percussion injury. *Glia* **49:**121–133.
Zeng GF, Pypaert M, and Slayman CL (2004) Epitope tagging of the yeast K^+ carrier trk2p demonstrates folding that is consistent with a channel-like structure. *J Biol Chem* **279:**3003–3013.
Zhou J and Sutherland ML (2004) Glutamate transporter cluster formation in astrocytic processes regulates glutamate uptake activity. *J Neurosci* **24:**6301–6306.

Address correspondence to: Dr. Marcus Rattray, University of Reading, Reading School of Pharmacy, 204 Hopkins Building, Whiteknights, Reading RG6 6UB, UK. E-mail: m.a.n.rattray@reading.ac.uk